Int. J. Heat Mass Transfer. Vol. 22, pp. 309–319

0017-9310/79/0201-0309 $02.00/0

A MODEL OF CONVECTOR HEATING FROM A FLAT PLATE

F. T. SMITH
Department of Mathematics, Imperial College, London S.W.7, England

and

D. S. RILEY
Department of Mathematics, University of Southampton, Southampton, SO9 5NH, England

(*Received* 11 *October* 1977 *and in revised form* 19 *July* 1978)

Abstract—The structure of the laminar flow and temperature distributions arising from finite ("strong") uniform hot-fluid injection on a vertical, horizontal or inclined flat plate is analysed. The viscous effects and regions of temperature change are convected a finite distance from the plate and are concentrated in a thin detached layer. Between this layer and the plate the blown fluid retains its plate temperature and is convected up and away from the convector plate. For only moderately strong blowing buoyancy forces tend to suppress the spreading of the blown fluid and it is found that the blown fluid spreads into a parabolically shaped region, except if the convector is nearly horizontal when the spreading abruptly increases. Conversely, for very strong blowing, the injectant penetrates a massive distance from the convector before the buoyancy effects force the injectant plume to gradually turn, contract and ultimately approach the vertical.

NOMENCLATURE

$\hat{A}$, $= (3\pi)^{2/3}2^{-5/3}$;
$\mathscr{F}_0$, value of $\Psi(x,\infty)$: see (2.7);
$\hat{f}$, similarity streamfunction in (4.4);
F, G, similarity streamfunction and temperature in region VI for the vertical convector;
f, g, similarity streamfunction and temperature in region II for the vertical convector;
$\hat{F}, \hat{G}, \hat{H}$, similarity streamfunction, temperature and pressure in region II for the horizontal convector;
g, gravity;
G_0, pressure at the outer edge of the injectant region;
Gr, Grashof number;
K, $= -\mathrm{d}x/\mathrm{d}R^*$ (in Section 5);
L, L_0, length of blowing and characteristic length scale;
p', p, pressure and non-dimensional pressure;
$p_0, \bar{P}, p^{(0)}$, values of p in regions I, II and III;
$\hat{p}_0, \tilde{p}_0, p_0^*, p_1, P_1, P_1^*$, values of p_0 in (4.1), (4.7), (4.10), (5.1), (5.5) and (5.10);
Pr, Prandtl number;
$R(x)$, position of layer IV;
$S, \hat{S}, \tilde{S}, S^*$, position of layer II, and its values in (4.1), (5.1) and (5.3);
T, T_w, T_∞, fluid temperature and its values at the convector and in the far field;
U_0, velocity at the outer edge of the injectant region;
(u', v'), velocity components;
(u, v), non-dimensional velocity components;
V_w, non-dimensional blowing velocity;
X, $= 2\alpha^{*3}x/\pi$ (in Section 6);
(x', y'), coordinates;
(x, y), non-dimensional coordinates;
$\bar{Y}, \tilde{Y}, Y, \hat{y}, y^*, \tilde{y}$, adjusted values of y in II, IV, V, (4.1), (5.3) and (5.1).

Greek symbols

α, inclination of convector to the vertical;
$\tilde{\alpha}$, $= (\pi/2 - \alpha)$;
α^*, $= V_w^{-2/3}\tilde{\alpha}$;
β, coefficient of cubical expansion of fluid;
ε, $= Gr^{-1/4}$;
ρ, density of fluid;
ν, kinematic viscosity of fluid;
κ, thermal diffusivity of fluid;
θ, non-dimensional temperature;
$\bar{\Theta}, \tilde{\Theta}$, values of θ in regions II and IV;
$\psi, \psi_0, \bar{\Psi}, \psi^{(0)}, \tilde{\Psi}, \Phi$, streamfunction and its adjusted values in regions I–V;
$\hat{\psi}_0, \tilde{\psi}_0, \psi_0^*, \psi_1, \Psi_1, \Psi_1^*$, adjusted values of ψ_0 in (4.1), (4.7), (4.10), (5.1), (5.5) and (5.10);
ξ, wall position of the streamline through (x, y) (in Section 3);
$\hat{\xi}, \eta, \hat{\eta}, \zeta$, similarity variables of (4.5a), (3.2a), (4.4) and (3.5);
$\tilde{\lambda}, \lambda$, constants from (3.2) and (3.6);
τ, $= 2\alpha^{*2}R^*/\pi$ (in Section 5).

1. INTRODUCTION

THE PROBLEM considered in this paper is that of the effects of strong uniform blowing on the (otherwise attached) free convection boundary layer on a heated semi-infinite vertical, inclined or horizontal flat plate. The plate is taken to be at a uniform

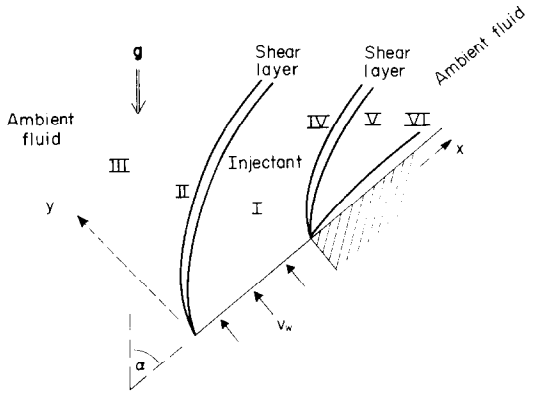

FIG. 1. Structure of the flow field (I–VI) produced by an inclined convector.

temperature and surrounded by a fluid which, far from the plate, is at a lower constant temperature and is at rest (Fig. 1). "Strong" here is taken to mean that the blowing velocity is so large that it is comparable with the maximum velocities induced throughout the flow field. Most previous investigations have been made into the problem of weak blowing, where "weak" signifies the minor blowing velocities that enable a conventional boundary-layer description to hold at large Grashof number. Sparrow and Cess [1] and Merkin [2], in particular, studied the effects of weak uniform blowing and uniform plate temperature. The former [1] adopted a coordinate expansion approach, which, unless many terms in the series are found, normally has the disadvantage of giving accurate results only for small values of the coordinate. Merkin [2] used a step-by-step numerical procedure to compute the solutions until the asymptotic solutions were attained. In the asymptotic solution, he found that there is a region next to the plate where the fluid is at the same temperature as the plate and viscosity can be neglected. His numerical solutions indicated an exact solution to this "injectant layer" and he was able to analyse the shear layer dividing this layer from the outer inviscid region. Finally, mention should be made of Clarke [3], who removed the Boussinesq approximation, made by the above authors, and solved the weak injection problem when the plate temperature is uniform but when the blowing is distributed non-uniformly in such a way that a similarity solution of the boundary-layer equations is available. Here again, as the weak blowing is increased, there is clear evidence of the viscous effects and temperature changes being blown far (on the boundary-layer scale) from the plate (see also [4]).

The present investigation, however, considers what we believe to be the more practical situation of strong uniform blowing at uniform temperature. Moreover, we extend the theory (which is confined to laminar flow) to consider the finite-length blowing problems for which the above similarity approaches cannot apply and to determine the influence of inclination of the plate. Possible applications of the theory are to the analysis of the convector heater, to the spreading of hot waste gases from buildings or to the blow-back from opened furnaces. We shall refer to the blowing plate as a "convector", for convenience.

In Section 2 the structures of the flow and the temperature fields during strong convection are derived from the full (Boussinesq) governing equations. Section 3 then discusses the vertical convector, where an exact solution of the main injectant layer flow proves possible for any strong blowing, with the blown fluid being confined to a parabolic shape. In contrast (Section 4.1), the horizontal convector produces a wider (though small) spread of the blown fluid when the blowing is only moderately strong. A study of the inclined convector (Section 4.2), also for moderately strong blowing, explains the transition between these two different spreads, for the spread is found to decrease sharply (to the parabolic shape) when the convector is only slightly inclined to the horizontal. At the other extreme, of very strong blowing (Section 5), progress is again possible. It is found that the injectant flow itself then sub-divides into three subzones, as the buoyancy force only gradually overcomes the inertia of the injectant, and the blown fluid penetrates a massive distance into the ambient fluid region before turning eventually to form a thin vertical plume. Further discussion is presented in Section 6.

2. GOVERNING EQUATIONS, AND THE STRUCTURE FOR STRONG CONVECTION

2.1. *The governing equations*

We consider a heated plate (at a uniform temperature T_w and inclined at an angle α to the vertical) occupying the region $y' = 0$, $x' > 0$ in a Boussinesq fluid which is quiescent and at temperature $T_\infty (< T_w)$ far from the plate; here (x', y') denote Cartesian coordinates. Through the section $0 < x' < L$ of the plate fluid of the same chemical type as the quiescent fluid is blown at temperature T_w. Steady conditions are assumed for the velocity components u', v', dynamic pressure p' and temperature T, and we let ρ be the density, ν the kinematic viscosity, κ the thermal diffusivity and β the coefficient of cubical expansion of the fluid, all of which are evaluated at the ambient temperature T_∞. Dimensionless variables are defined by

$$(x, y) = L_0^{-1}(x', y'), \quad \theta = (T - T_\infty)/(T_w - T_\infty)$$
$$(u, v) = [g\beta(T_w - T_\infty)L_0]^{-1/2}(u', v') \qquad (2.1)$$
$$p = [\rho g\beta(T_w - T_\infty)L_0]^{-1}p'$$

where g denotes gravity and L_0 is a reference length (equal to $\frac{1}{2}L$, say, when L is finite). With a stream function $\psi (u = \partial\psi/\partial y,\ v = -\partial\psi/\partial x)$ introduced, the equations of motion and thermal convection become

$$\frac{\partial\psi}{\partial y}\frac{\partial^2\psi}{\partial x\,\partial y} - \frac{\partial\psi}{\partial x}\frac{\partial^2\psi}{\partial y^2} = -\frac{\partial p}{\partial x} + \theta\cos\alpha + \varepsilon^2\nabla^2\left(\frac{\partial\psi}{\partial y}\right) \qquad (2.2a)$$

$$-\frac{\partial\psi}{\partial y}\frac{\partial^2\psi}{\partial x^2}+\frac{\partial\psi}{\partial x}\frac{\partial^2\psi}{\partial x\,\partial y}$$

$$=-\frac{\partial p}{\partial y}+\theta\sin\alpha-\varepsilon^2\nabla^2\left(\frac{\partial\psi}{\partial x}\right) \quad (2.2b)$$

$$\frac{\partial\psi}{\partial y}\frac{\partial\theta}{\partial x}-\frac{\partial\psi}{\partial x}\frac{\partial\theta}{\partial y}=\frac{\varepsilon^2}{Pr}\nabla^2\theta. \quad (2.2c)$$

Here $\varepsilon = Gr^{-1/4}$, $Gr = L_0^3 g\beta(T_w - T_\infty)/\nu^2$ is the Grashof number, and Pr is the Prandtl number ν/κ. The boundary conditions are

$$\theta = 1, \quad \frac{\partial\psi}{\partial y} = 0, \quad \psi = -V_w x \quad \text{on } y = 0 \text{ for } 0 < x < L/L_0 \quad (2.3a)$$

$$\theta = 1, \quad \frac{\partial\psi}{\partial y} = 0, \quad \psi = -V_w L/L_0 \quad \text{on } y = 0 \text{ for } x > L/L_0 \quad (2.3b)$$

$$\theta, p, \psi \to 0 \quad \text{as } y \to \infty \text{ (and upstream).} \quad (2.3c)$$

The dimensionless transpiration velocity is denoted here by V_w.

2.2. *The structure for strong convection*

Our interest is in the effects of strong blowing [$V_w = O(1)$] at large Grashof number ($\varepsilon \ll 1$). We propose the following structure for the flow and thermal fields (see Fig. 1). First, viscous effects are blown a finite distance away from the wall to form a viscous shear layer (II). Between II and the wall a zone (the injectant region I) of an inviscid but rotational kind is left, containing only blown fluid which stays at the uniform injectant temperature ($\theta = 1$). The lack of temperature change in I is due to the conservation of temperature along the streamlines of I. Instead, the fluid temperature falls to its ambient value ($\theta = 0$) through the thin layer II, outside of which (in zone III) a relatively slow motion is induced because of entrainment.

In I,

$$\psi = \psi_0 + O(\varepsilon), \quad p = p_0 + O(\varepsilon), \quad \theta = 1 \quad (2.4)$$

where, from (2.2), ψ_0 and p_0 satisfy

$$\frac{\partial\psi_0}{\partial y}\frac{\partial^2\psi_0}{\partial x\,\partial y}-\frac{\partial\psi_0}{\partial x}\frac{\partial^2\psi_0}{\partial y^2}=-\frac{\partial p_0}{\partial x}+\cos\alpha \quad (2.5a)$$

$$-\frac{\partial\psi_0}{\partial y}\frac{\partial^2\psi_0}{\partial x^2}+\frac{\partial\psi_0}{\partial x}\frac{\partial^2\psi_0}{\partial x\,\partial y}=-\frac{\partial p_0}{\partial y}+\sin\alpha. \quad (2.5b)$$

Also, ψ_0 satisfies the boundary conditions in (2.3a), supplemented by

$$\psi_0 = 0 \quad \text{on} \quad y = S(x) \quad (2.5c)$$

$$p_0 = 0 \quad \text{on} \quad y = S(x). \quad (2.5d)$$

Here $y = S(x)$ is the unknown shape of the bounding streamline ($\psi = 0$) between the blown and the original fluid, while (2.5d) is required to reduce the pressure to a small value consistent with the low velocities promoted in region III. In II, $y = S(x) + \varepsilon\bar{Y}$, $\psi = \varepsilon\bar{\Psi}$, $p = \varepsilon\bar{P}$ and $\theta = \bar{\Theta}$ to leading order, with (2.2) yielding

$$\frac{\partial\bar{\Psi}}{\partial\bar{Y}}\frac{\partial^2\bar{\Psi}}{\partial x\,\partial\bar{Y}}-\frac{\partial\bar{\Psi}}{\partial x}\frac{\partial^2\bar{\Psi}}{\partial\bar{Y}^2}$$

$$=S'(x)\frac{\partial\bar{P}}{\partial\bar{Y}}+\bar{\Theta}\cos\alpha+[1+S'^2]\frac{\partial^3\bar{\Psi}}{\partial\bar{Y}^3} \quad (2.6a)$$

$$S''\left(\frac{\partial\bar{\Psi}}{\partial\bar{Y}}\right)^2=-(1+S'^2)\frac{\partial\bar{P}}{\partial\bar{Y}}+\bar{\Theta}(\sin\alpha+S'\cos\alpha) \quad (2.6b)$$

$$\frac{\partial\bar{\Psi}}{\partial\bar{Y}}\frac{\partial\bar{\Theta}}{\partial x}-\frac{\partial\bar{\Psi}}{\partial x}\frac{\partial\bar{\Theta}}{\partial\bar{Y}}=Pr^{-1}(1+S'^2)\frac{\partial^2\bar{\Theta}}{\partial\bar{Y}^2}. \quad (2.6c)$$

The boundary conditions are

$$\bar{\Theta}\to 1, \quad \frac{\partial\bar{\Psi}}{\partial\bar{Y}}\to U_0(x), \quad \frac{\partial\bar{P}}{\partial\bar{Y}}\to G_0(x) \quad \text{as } \bar{Y}\to-\infty \quad (2.6d)$$

$$\bar{\Theta}\to 0, \quad \frac{\partial\bar{\Psi}}{\partial\bar{Y}}\to 0, \quad \bar{P}\to 0 \quad \text{as } \bar{Y}\to+\infty \quad (2.6e)$$

where $U_0(x)$, $G_0(x)$ are the values of $\partial\psi_0/\partial y$ and $\partial p_0/\partial y$ respectively, at $y = S(x)-$ in I. Thus (2.6d) merges II with I, while conditions (2.6e) match II to the exterior flow region III, wherein $\psi = \varepsilon\psi^{(0)}$, $p = \varepsilon^2 p^{(0)}$ to leading order, and $\theta = 0$. Hence in III, since the vorticity is zero at infinity, (2.2) reduce to solving $\nabla^2\psi^{(0)} = 0$, with

$$\partial\psi^{(0)}/\partial x, \ \partial\psi^{(0)}/\partial y \to 0 \quad \text{at infinity} \quad (2.7a)$$

$$\psi^{(0)} = 0 \quad \text{on } y = 0 \text{ for } x < 0 \quad (2.7b)$$

$$\psi^{(0)} = \mathscr{F}_0(x) \quad \text{on } y = S(x) \text{ for } x > 0, \quad (2.7c)$$

$\mathscr{F}_0(x)$ being the value of $\bar{\Psi}$ for $\bar{Y}\to\infty$.

When the blowing length L is finite, another (thin) viscous shear layer (IV) is expected to emanate from the end-point $x = L/L_0$ and to occupy a position $y = R(x)$, say, for $x > L/L_0$. The boundary conditions on the dividing streamline $y = R(x)$, as far as region I is concerned, are analogous to (2.5c,d) and are

$$\psi_0 = -V_w L/L_0, \quad p_0 = 0 \quad \text{on} \quad y = R(x). \quad (2.8)$$

The actual structure of layer IV surrounding $y = R(x)$ is similar to that of II above, so that again a mass entrainment, from the original fluid, is necessary to maintain it. Hence a relatively slow motion (similar to that in III) is provoked in the zone V lying between IV and the plate. This flow is also affected by the shear layer VI which grows adjacent to the plate in $x > L/L_0$ and which also entrains fluid from zone V.

Figure 1 illustrates the above structure for strong convection. Below we set out to solve the first order problems in each zone I–III for different values of α and various values of V_w.

3. THE VERTICAL CONVECTOR

It happens that when $\alpha = 0$ the solution of (2.5a–d) for region I is also an exact solution of the complete governing equations (2.2), namely

$$\psi = \frac{y^2}{2V_w} - V_w x, \quad p = 0, \quad \theta = 1. \tag{3.1}$$

This was also observed by Merkin [2] in the weak injection case. Thus the streamlines are the parabolas $y = [2(x-\xi)]^{1/2}V_w$, where $x = \xi (0 < \xi < L/L_0)$ is the point at which the streamline through (x, y) emerged from the plate $y = 0$, and the bounding streamline has $S(x) = V_w(2x)^{1/2}$.

The solution (3.1) holds for any strong blowing V_w. However, a numerical treatment of (2.6a–c) for the shear layer II seems necessary in general. An exception occurs if $V_w \ll 1$ ("moderately strong" blowing, with which the rest of Section 3 is concerned), when the terms involving the derivatives of S may be neglected to first order. Then the shear layer solution has the similarity form (c.f. [5])

$$\bar{\Psi} = (4x)^{3/4} f(\eta), \quad \bar{\Theta} = g(\eta), \quad \bar{P} = 0 \qquad \text{where } \eta = \bar{Y}/(4x)^{1/4} \tag{3.2a}$$

and f and g satisfy

$$f''' + 3ff'' - 2f'^2 + g = 0, \quad g'' + 3Prfg' = 0 \tag{3.2b}$$

with $f'(\infty) = g(\infty) = 0$, $f'(-\infty) = 2^{-1/2}$, $g(-\infty) = 1$, from (2.6a–c), since here $U_0(x) = (2x)^{1/2}$. The numerical solution [2] gives $f(\infty) = \tilde{\lambda}/2(2)^{1/2}$, where $\tilde{\lambda} = 1.539$ if $Pr = 1$.

For the external flow in III, we have in (2.7c) that $\mathscr{F}_0(x) = \tilde{\lambda}x^{3/4}$ and that, since V_w is small, $S(x)$ may be replaced by zero to lowest order in V_w. Hence

$$\psi^{(0)} = 2^{1/2}\tilde{\lambda}(x^2+y^2)^{3/8}\cos\left[\frac{3}{4}\tan^{-1}\left(\frac{x}{y}\right) - \frac{\pi}{8}\right]. \tag{3.3}$$

If the blowing length L is infinite, (3.1)–(3.3) complete the first order solution throughout the flow and temperature fields. If L is finite (so that $L_0 = \frac{1}{2}L$), regions IV, V and VI also need consideration. We have, in IV, $Y = R(x) + \varepsilon\tilde{Y}$, where $R(x) = [2(x - L/L_0)]^{1/2}V_w$ from (3.1) and $\tilde{Y}$ is $O(1)$. Also, $\psi = -V_w(L/L_0) + \varepsilon\tilde{\Psi}$, $\theta = \tilde{\Theta}$, $p = 0$ to leading orders and the controlling equations for $\tilde{\Psi}$, $\tilde{\Theta}$ are again (2.6) effectively but subject to the matching conditions

$$\left.\begin{aligned} &\tilde{\Psi} \sim [2(x - L/L_0)]^{1/2}\tilde{Y}, \ \tilde{\Theta} \to 1 \text{ as } \tilde{Y} \to \infty \\ &\frac{\partial\tilde{\Psi}}{\partial\tilde{Y}} \text{ and } \tilde{\Theta} \to 0 \text{ as } \tilde{Y} \to -\infty \end{aligned}\right\}. \tag{3.4a}$$

Replacing $\tilde{\Psi}$ by $-\bar{\Psi}$, $\tilde{\Theta}$ by $\bar{\Theta}$, $\tilde{Y}$ by $-\bar{Y}$ and $(x - L/L_0)$ by x, we recover the problem of layer II. Therefore $\bar{\Psi}(x, -\infty)$, which is related to the mass of fluid entrained into IV, satisfies

$$\bar{\Psi}(x, -\infty) = -[4(x - L/L_0)]^{3/4} f(\infty) = -\tilde{\lambda}(x - L/L_0)^{3/4} \tag{3.4b}$$

when V_w is small. This gives the required matching condition for the inviscid irrotational zone V. However, before we can consider V, we first need to analyse the free convection boundary layer VI growing from $x = L/L_0$, since this also contributes an $O(\varepsilon)$ term to the matching. The problem in VI is governed by the classical Pohlhausen equations; if

$$\psi = -V_w\frac{L}{L_0} + \varepsilon\left[4\left(x - \frac{L}{L_0}\right)\right]^{3/4} F(\zeta), \qquad \theta = G(\zeta), \quad \zeta = \frac{y}{\varepsilon\left[4\left(x - \frac{L}{L_0}\right)\right]^{1/4}}, \tag{3.5}$$

then the governing equations for F and G are:

$$\left.\begin{aligned} &F''' - 2F'^2 + 3FF'' + G = 0, \\ &G'' + 3PrFG' = 0 \end{aligned}\right\} \tag{3.6}$$

with $F(0) = F'(0) = 0$, $G(0) = 1$ and $F'(\infty) = G(\infty) = 0$. Ostrach [6] has solved these equations for a wide range of Prandtl number; in particular, for $Pr = 1$, he found that $F(\infty) = 0.5194$. So in general, for $\zeta \gg 1$,

$$\psi \approx -V_w\frac{L}{L_0} + \varepsilon\lambda(x - L/L_0)^{3/4} + O(\varepsilon)$$

where $\lambda = 4^{3/4}F(\infty) > 0$. Since both λ and $\tilde{\lambda}$ are positive, fluid is entrained from region V into both the free convection layers IV and VI.

Neglecting terms of $O(\varepsilon)$, we have in V that

$$\psi = -V_w\frac{L}{L_0} + \varepsilon\Phi \text{ (and } \theta \equiv 0),$$

where Φ satisfies Laplace's equation with

$$\left.\begin{aligned} &\Phi(x, 0+) = \lambda\left(x - \frac{L}{L_0}\right)^{3/4}: \quad x > L/L_0 \\ &\Phi[x, R(x)-] = \bar{\Psi}(x, -\infty): \quad x > L/L_0 \end{aligned}\right\} \tag{3.7}$$

and zero vorticity upstream. The solution for Φ is obtainable when V_w is small since then (3.4b) may be used in (3.7). A small region of adjustment persists near $x = L/L_0$, $y = 0$, wherein $[x - (L/L_0)]$ and y are both $O(V_w^2)$, but for $[x - (L/L_0)]$ finite and positive we scale $y = V_w Y$, so that $0 < Y < (2)^{1/2}[x - (L/L_0)]^{1/2}$ in V and Φ satisfies $\partial^2\Phi/\partial Y^2 = 0$ to leading order. Hence the solution satisfying (3.7) is

$$\Phi = \lambda\left(x - \frac{L}{L_0}\right)^{3/4} - (\lambda + \tilde{\lambda})\frac{Y\left(x - \frac{L}{L_0}\right)^{1/4}}{2^{1/2}}. \tag{3.8}$$

Thus the entire first order solution is again obtainable, for finite values of L and small values of V_w. Figure 2 gives a sketch of the flow pattern induced by the vertical convector.

We turn next (Sections 4 and 5) to solutions for nonzero values of α, taking L to be infinite, for convenience, in Section 4. We concentrate mostly on the injectant zone I since, as the exact solution (3.1)

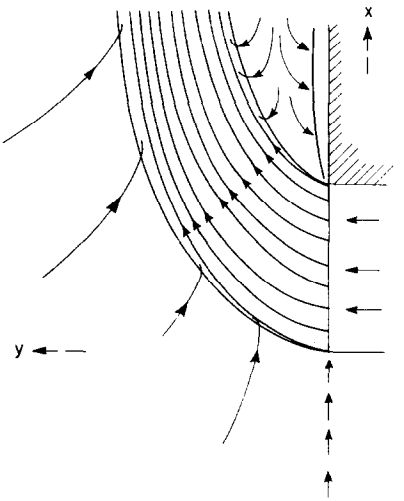

FIG. 2. Sketch of the streamlines induced by a vertical convector.

above has shown, the features of the other zones II–VI follow fairly readily from those of I. Section 4 considers moderately strong blowing (V_w small) again, while Section 5 considers "very strong" blowing (V_w large).

4. THE HORIZONTAL OR INCLINED CONVECTOR FOR MODERATELY STRONG BLOWING

4.1. *The horizontal case*

For $\alpha = \pi/2$, a numerical treatment of (2.5) in the injectant region I also seems necessary to determine the bounding streamline shape $S(x)$ and slip velocity $U_0(x)$ when V_w is $O(1)$. However, as in the case of the vertical convector, progress can be made when $V_w \ll 1$. Then the solution in I has the expanded form (for x finite)

$$\psi_0 = V_w\hat{\psi}_0 + O(V_w^{4/3}),\quad p_0 = V_w^{2/3}\hat{p}_0 + O(V_w),$$
$$S(x) = V_w^{2/3}\hat{S}(x) + O(V_w) \tag{4.1}$$

with $y = V_w^{2/3}\hat{y}$, where the leading terms satisfy, from (2.5), the non-linear but simplified equations

$$\frac{\partial\hat{\psi}_0}{\partial\hat{y}}\frac{\partial^2\hat{\psi}_0}{\partial x\,\partial\hat{y}} - \frac{\partial\hat{\psi}_0}{\partial x}\frac{\partial^2\hat{\psi}_0}{\partial\hat{y}^2} = -\frac{\partial\hat{p}_0}{\partial x} \tag{4.2a}$$

$$0 = -\frac{\partial\hat{p}_0}{\partial\hat{y}} + 1 \tag{4.2b}$$

with

$$\hat{\psi}_0 = 0 \text{ on } \hat{y} = \hat{S}(x),\ \hat{\psi}_0 = -x \text{ on } \hat{y} = 0 \tag{4.2c}$$

$$\hat{p}_0 = 0 \text{ on } \hat{y} = \hat{S}(x). \tag{4.2d}$$

From (4.2b) and (4.2d), $\hat{p}_0 = \hat{y} - \hat{S}(x)$ and on substituting this result into (4.2a), we arrive at the result (from [7])

$$\hat{S}(x) = 2^{-1/2}\int_0^x \frac{d\xi}{[\hat{S}(x) - \hat{S}(\xi)]^{1/2}}. \tag{4.3}$$

The solution is $\hat{S}(x) = \hat{A}x^{2/3}$ where $\hat{A} = (3\pi)^{2/3}2^{-5/3}$. Using this we find, from (4.2), that the flow in I is given by

$$\hat{\psi}_0 = x\hat{f}(\hat{\eta}) \quad \text{where} \quad \hat{\eta} = \hat{y}/x^{2/3} \tag{4.4}$$

and

$$\frac{2}{3}(2\hat{A})^{1/2}\hat{\eta} = \frac{\pi}{2} + (-\hat{f})^{1/3} \times [1 - (-\hat{f})^{2/3}]^{1/2} - \sin^{-1}[(-\hat{f})^{1/3}].$$

It is noteworthy that, if the injection velocity is $\propto x^m$ rather than constant, the consequent analogue of (4.3) yields $\hat{S} \propto x^{2/3(m+1)}$ which is consistent with the result in [4].

The free convection layer II is then described by a similarity solution:

$$\bar{\Psi} = V_w^{1/6}x^{2/3}\hat{F}(\hat{\xi}),\quad \bar{\Theta} = \hat{G}(\hat{\xi}),$$
$$\bar{P} = V_w^{-1/6}x^{1/3}\hat{H}(\hat{\xi}):\quad \hat{\xi} = \frac{V_w^{1/6}\bar{Y}}{x^{1/3}} \tag{4.5a}$$

to leading order in V_w. Here $\hat{F}$, $\hat{G}$, $\hat{H}$ satisfy

$$\left.\begin{aligned} &3\hat{F}''' + 2\hat{F}\hat{F}'' - (\hat{F}')^2 + 2\hat{A}\hat{H}' = 0 \\ &\hat{H}' - \hat{G} = 0 \\ &3Pr^{-1}\hat{G}'' + 2\hat{F}\hat{G}' = 0 \end{aligned}\right\} \tag{4.5b}$$

from (2.6), with $\hat{F}'(\infty) = 0$, $\hat{F}'(-\infty) = (2\hat{A})^{1/2}$, $\hat{G}(-\infty) = 1$, $\hat{G}(\infty) = 0$, $\hat{H}'(-\infty) = 1$ and $\hat{H}(\infty) = 0$. A numerical solution (see Fig. 3) yields the value $\hat{F}(\infty) = 1.7253$ for $Pr = 1$.

Finally, for the external flow in III, we find that

$$\psi^{(0)} = V_w^{1/6}\frac{2\hat{F}(\infty)}{3^{1/2}}(x^2 + y^2)^{1/3} \times \cos\left[\frac{2}{3}\tan^{-1}\left(\frac{x}{y}\right) - \frac{\pi}{6}\right] + O(V_w^{5/6}) \tag{4.6}$$

which satisfies (2.7c) in its limiting form for small V_w:

$$\psi^{(0)} = V_w^{1/6}x^{2/3}\hat{F}(\infty) \text{ on } y = 0.$$

Having found the solution for the horizontal and vertical convectors when V_w is small, we consider next the inclined convector $[0 < \alpha < \pi/2]$. Particularly intriguing is the property that $S(x) \propto x^{2/3}$ for the horizontal convector, whereas $S(x) \propto x^{1/2}$ for the vertical one, so that an investigation of the transition when $0 < \alpha < \pi/2$ between these two growth rates is required. Before discussing the range $0 < \alpha < \pi/2$, however, we observe that when L is infinite the solutions for V_w small and x finite are equivalent to solutions for V_w finite and x large. For the factor V_w in (2.5) can then be scaled out of the governing problem and it is seen that the results above, and in Section 5 below, correspond to asymptotic downstream results for $V_w^{-2}x \gg 1$. Hence the small-V_w solutions (for any α) are non-uniform in a small region where x, y are $O(V_w^2)$, within which the full equations (2.5a,b) are retrieved. This facet explains the simplicity of the solution (4.4), for instance. In the more realistic case where L is finite, however, this reinterpretation does not hold. We note too that, for the horizontal convector only, some symmetry is expected about the line $x = L/2L_0$ if L is finite.

4.2. *The inclined case*

The character of the flow field for the inclined

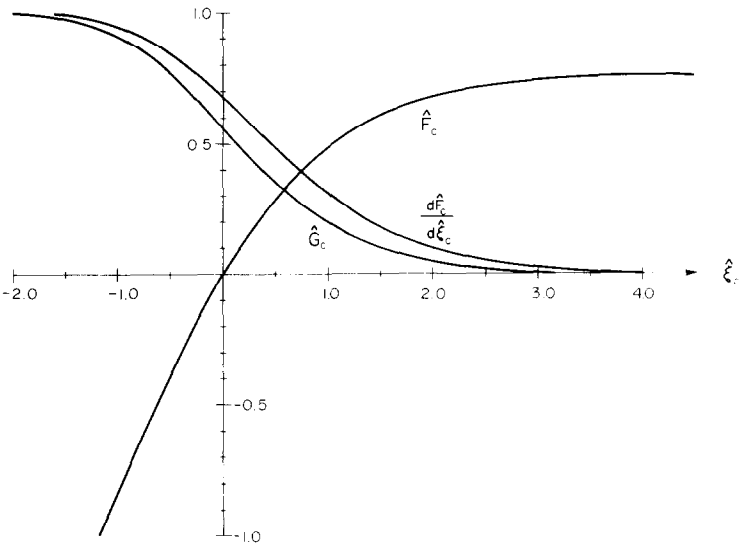

FIG. 3. Calculated solution curves for (4.5a,b) when $Pr = 1$; here $\hat{F}_c = \hat{F}/3^{1/2}(2\hat{A})^{1/4}$, $\hat{G}_c = \hat{G}$, $\hat{\xi}_c = 3^{-1/2}(2\hat{A})^{1/4}\hat{\xi}$, and $\hat{F}_c(\infty) = 0.7694$.

convector depends on whether $0 \leqslant \alpha < \pi/2$ or $\alpha \approx \pi/2$. For we find that a fast transition occurs, between the behaviours $S \propto x^{1/2}$ and $S \propto x^{2/3}$, when the convector plate is just slightly inclined to the horizontal.

First, if $0 \leqslant \alpha < \pi/2$, then when $V_w \ll 1$

$$\psi_0 = V_w\tilde{\psi}_0,\ p_0 = V_w\tilde{p}_0,\ S = V_w\tilde{S} \tag{4.7}$$

to leading order in I, with $y = V_w\tilde{y}$. The governing equations in I yield the solution (as in Section 3)

$$\tilde{S}(x) = \left(\frac{2x}{\cos\alpha}\right)^{1/2} \tag{4.8}$$

so that $S(x) \propto x^{1/2}$ for all these values of α. The joining with the (exact) vertical plate solution (Section 3) as $\alpha \to 0$ is regular, but no direct match exists with the horizontal case as $\alpha \to \pi/2$, since there $S(x) \propto x^{2/3}$. Second, therefore, there must be a singular regime when $(\pi/2-\alpha)$ is small, a fact suggested also by the $(\cos\alpha)^{-1/2}$ factor in (4.8).

If we write $\alpha = \pi/2-\tilde{\alpha}$ with $\tilde{\alpha}$ small, then (4.8) becomes invalid when $\tilde{\alpha}$ is $O(V_w^{2/3})$ ($\tilde{\alpha} = V_w^{2/3}\alpha^*$, say), since then S in (4.7) and in (4.1) achieve comparable orders of magnitude. When α^* is $O(1)$,

$$\psi_0 = V_w\psi_0^*,\ p_0 = V_w^{2/3}p_0^*,\ S = V_w^{2/3}S^* \tag{4.9}$$

with $y = V_w^{2/3}y^*$, to leading order in I and (2.5) yields

$$p_0^* = y^* - S^*(x) \tag{4.10a}$$

$$\frac{\partial\psi_0^*}{\partial y^*}\frac{\partial^2\psi_0^*}{\partial x\,\partial y^*} - \frac{\partial\psi_0^*}{\partial x}\frac{\partial^2\psi_0^*}{\partial y^{*2}} = \alpha^* + \frac{dS^*}{dx}. \tag{4.10b}$$

Here (4.10a) stems from integration of the y-momentum equation, while (4.10b) follows from the x-momentum equation with p_0^* substituted from (4.10a). Thus the effective pressure gradient driving the injectant layer I is the sum of the buoyancy force (α^*) and the convective force ($S^{*\prime}$). The boundary conditions on (4.10b) are $\psi_0^* = 0$ on $y^* = S^*$ and $\psi_0^* = -x$, $\partial\psi_0^*/\partial y^* = 0$ on $y^* = 0$. The solution, from [7], gives the integral equation

$$S^*(x) = 2^{-1/2}\int_0^x \frac{d\xi}{[S^*(x)-S^*(\xi)+\alpha^*(x-\xi)]^{1/2}} \tag{4.11a}$$

to determine $S^*(x)$. This may be manipulated to yield x in terms of S^*, as follows. Setting $R^* = S^* + \alpha^*x$, we treat $dx/dR^*[= -K(R^*)]$ as a function of R^* in (4.11a), so that

$$R^* + \alpha^*\int_0^{R^*} K(t)\,dt = -2^{-1/2}\int_0^{R^*} \frac{K(q)\,dq}{(R^*-q)^{1/2}}. \tag{4.11b}$$

Integration of the RHS by parts and then differentiation with respect to R^* produces

$$1 + \alpha^*K(R^*) = -2^{-1/2}\int_0^{R^*} \frac{K'(\bar{q})\,d\bar{q}}{(R^*-\bar{q})^{1/2}}. \tag{4.11c}$$

Upon substituting for K from (4.11c) into (4.11b), and putting $q = R^*\sin^2\phi + \bar{q}\cos^2\phi$ in the resultant double integral, we obtain

$$-2^{1/2}\left\{R^* + \alpha^*\int_0^{R^*} K(t)\,dt\right\} = -\frac{2}{\alpha^*}R^{*1/2} - \frac{\pi}{\alpha^*2^{1/2}}K(R^*) \tag{4.11d}$$

which, on integration, yields the relation

$$X = \tau - 2(\tau/\pi)^{1/2} + e^{\tau}\,\mathrm{erf}(\tau^{1/2}) + 1 - e^{\tau}. \tag{4.12}$$

Here $X = 2\alpha^{*3}x/\pi$, $\tau = 2\alpha^{*2}R^*/\pi$ and we have assumed that $R^*(0) = 0$.

The relation (4.12) accounts for the transition from the horizontal convector form ($S \propto x^{2/3}$, holding when $\alpha^* \ll 1$) to the inclined convector form ($S \propto x^{1/2}$, holding when $\alpha^* \gg 1$). When $\alpha^* \ll 1$, (4.12) gives [when $x = O(1)$]

$$S^* \approx \hat{A}x^{2/3} + \alpha^*\left[\frac{3\pi}{16} - 1\right]x + O(\alpha^{*2}) \tag{4.13}$$

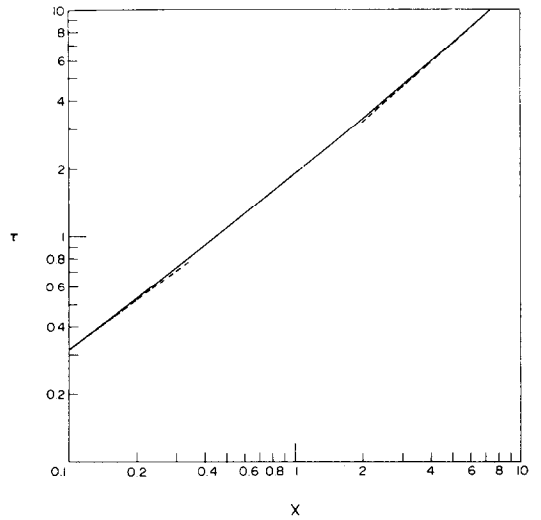

FIG. 4. Graph of the solution (4.12) for τ vs X. The dashed lines indicate the asymptotes (4.13) and (4.14).

matching with the results of Section 4.1, while for $\alpha^* \gg 1$ and $x = O(1)$,

$$S^* \approx \left(\frac{2x}{\alpha^*}\right)^{1/2} + \alpha^{*-2}\left(1-\frac{\pi}{2}\right) + O(\alpha^{*-7/2}) \quad (4.14)$$

which continues into (4.8). The solution of (4.12) for general values of α^*, obtained numerically, is drawn in Fig. 4.

The free convection layer (II) flows and temperature distributions follow similar lines to those presented in Sections 3 and 4.1, as do the entrainment induced exterior flows III.

5. THE HORIZONTAL OR INCLINED CONVECTOR FOR VERY STRONG BLOWING

When V_w is large analytical progress is again possible, with the injectant region I itself now subdividing into three subzones ⓐ, ⓑ, ⓒ, considered in turn below. We concentrate on the finite blowing length problem, choosing $L_0 = L/2$; the structure ⓐ, ⓑ, ⓒ is shown diagrammatically in Fig. 5.

5.1. *Subzone* ⓐ

This subzone forms the initial, fairly long, part of the blown region, in which the blown fluid travels almost straight from the plate (Fig. 5) because the inertia of the very strong convection dominates over the buoyancy forces. In ⓐ, y is $O(1)$ and

$$\psi_0 = -V_w x + V_w^{-1}\psi_1 + \ldots, \quad p_0 = p_1 + \ldots. \quad (5.1)$$

Also, for V_w large it proves best to consider the dividing streamlines, emanating from $x = 0$ and $x = 2$, as functions of y rather than x, i.e. $x = \bar{S}(y)$ and $x = 2 + \bar{R}(y)$ correspond to the curves $y = S(x)$ and $y = R(x)$ of Section 2 respectively. Then, in ⓐ,

$$\begin{aligned} \bar{S}(y) &= V_w^{-2}S_1(y) + \ldots \text{(a)}, \\ \bar{R}(y) &= V_w^{-2}R_1(y) + \ldots \text{(b)} \end{aligned} \quad (5.2)$$

so that the dividing streamlines are nearly straight. From (5.1) and (2.5a,b), $u_1 = \partial\psi_1/\partial y$ satisfies $\nabla^2 u_1 = 0$. Also, from (5.2) and (2.5c,d), (2.8), the boundary conditions on u_1 are $\partial u_1/\partial x = -\sin\alpha$ at $x = 0,2$ and $u_1 = 0$ at $y = 0$ (together with boundedness as $y \to \infty$). The solution for u_1 is therefore

$$u_1 = (1-x)\sin\alpha + \sum_0^\infty A_n \cos\left[(2n+1)\frac{\pi x}{2}\right] \times \exp\left[-(2n+1)\frac{\pi y}{2}\right] + Cy \quad (5.3a)$$

where

$$A_n = -8\sin\alpha/\pi^2(2n+1)^2 \quad (n = 0,1,2,\ldots) \quad (5.3b)$$

but the constant C is as yet undetermined. The continuity and momentum equations now yield

$$\left.\begin{aligned} \psi_1 &= (1-x)y\sin\alpha + \tfrac{1}{2}Cy^2 \\ &\quad + \frac{2}{\pi}\sum_0^\infty \frac{A_n}{(2n+1)}\cos\left[(2n+1)\frac{\pi x}{2}\right] \\ &\quad \times \left\{1 - \exp\left[-(2n+1)\frac{\pi y}{2}\right]\right\} \\ p_1 &= (\cos\alpha - C)x + \sum_0^\infty A_n \sin\left[(2n+1)\frac{\pi x}{2}\right] \\ &\quad \times \exp\left[-(2n+1)\frac{\pi y}{2}\right] \end{aligned}\right\} \quad (5.4)$$

where the conditions $\psi_1 = 0$ at $y = 0$ and $p_1 = 0$ at $x = 0$ [from (2.5d)] have been applied. But, from (2.8) and (5.2), we also require $p_1 = 0$ at $x = 2$. Therefore $C = \cos\alpha$, and the solution in ⓐ is complete. The almost straight dividing streamline shapes of (5.2) can be determined by applying $\psi_0 = 0$ on (5.2a) and $\psi_0 = -2V_w$ on (5.2b). However, the expansions (5.1) become invalid when y grows to

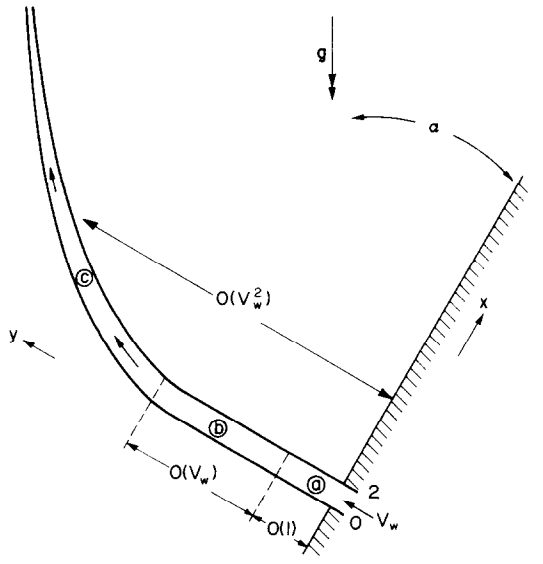

FIG. 5. Schematic diagram of the injectant flow structure (ⓐ–ⓑ–ⓒ) during very strong blowing ($V_w \gg 1$) from an inclined convector.

$O(V_w)$ [since then ψ_1 in (5.4) becomes $O(V_w^2)$, invalidating (5.1)] and so a new subzone ⓑ occurs then, far from the convector.

5.2. *Subzone* ⓑ

In ⓑ we find that the first significant bending (upwards) of the injectant takes place (Fig. 5), due to the gradual influence of the buoyancy forces on the very strongly convected fluid. However, the injectant width remains virtually unaltered during subzone ⓑ. Thus, in ⓑ, the expansions, implied by Section 5.1, and further considerations of consistency, are

$$\psi_0 = V_w(-x+\tfrac{1}{2}Y_1^2\cos\alpha)+\Psi_1+\ldots, \qquad p_0 = V_w^{-1}P_1+\ldots \tag{5.5}$$

where $y = V_w Y_1$ and $Y_1 = O(1)$. Also, now

$$\bar{S} = \tilde{S}_1 + V_w^{-1}\tilde{S}_2+\ldots\text{(a)}, \qquad \bar{R} = \tilde{R}_1 + V_w^{-1}\tilde{R}_2+\ldots.\text{(b)}. \tag{5.6}$$

The governing equations become the linear system

$$\frac{\partial U_1}{\partial x}+\frac{\partial V_1}{\partial Y_1}=0,$$

$$Y_1\cos\alpha\frac{\partial U_1}{\partial x}+V_1\cos\alpha+\frac{\partial U_1}{\partial Y_1}=-\frac{\partial P_1}{\partial x}, \tag{5.7}$$

$$Y_1\cos\alpha\frac{\partial V_1}{\partial x}+\frac{\partial V_1}{\partial Y_1}=\sin\alpha$$

from (2.5a,b) with (5.5) (here $U_1 = \partial\Psi_1/\partial Y_1$, $V_1 = -\partial\Psi_1/\partial x$). The boundary conditions on (5.7) require matching with subzone ⓐ as $Y_1 \to 0$ and $P_1 = 0$ at $x = \tilde{S}_1, \tilde{R}_1$ from (2.5d), (2.8). The solution is

$$V_1 = Y_1\sin\alpha, \quad U_1 = (1-x)\sin\alpha, \qquad \Psi_1 = (1-x)Y_1\sin\alpha, \quad P_1 = 0, \tag{5.8}$$

therefore. Hence, applying $\psi_0 = 0$, $-2V_w$ at $x = \bar{S}$, $2+\bar{R}$ respectively, we have

$$\tilde{S}_1 = \tilde{R}_1 = \tfrac{1}{2}Y_1^2\cos\alpha, \qquad \tilde{S}_2 = \tilde{R}_2 = (1-\tfrac{1}{2}Y_1^2\cos\alpha)Y_1\sin\alpha, \tag{5.9}$$

implying the gradual bending upwards (but with unchanging injectant width) referred to above.

Clearly, a further breakdown of the expansions will occur when Y_1 increases now, because of the growth of Ψ_1 in (5.8) and the form of ψ_0 in (5.5) [see also (5.6) with (5.9)]. The breakdown happens when Y_1 is $O(V_w)$, or y is $O(V_w^2)$, which leads us to the third, and final, subzone of the injectant region, much further from the convector.

5.3. *Subzone* ⓒ

This final stage of the injectant motion involves both the complete turning of the blown fluid, from its original direction (normal to the inclined plate) to the vertically upward direction, and a considerable contraction of the injectant width as the vertical direction is approached (Fig. 5). The turning is completed as the buoyancy forces eventually overwhelm the initial impact of the very strong convection. Analytically, it proves convenient to use the displaced coordinate $\bar{x} = x-\bar{R}(y)$ (centred on the upper dividing streamline) rather than x in the injectant region. Then, in ⓒ, where $y = V_w^2 Z$ and Z, $\bar{x}$ are $O(1)$,

$$\psi_0 = V_w\Psi_1^*+\ldots, \quad p_0 = P_1^*+\ldots \tag{5.10}$$

and

$$\bar{R}(y) = V_w^2 R_1^*(Z)+\ldots\text{(a)}, \qquad \bar{S}(y) = \bar{R}(y)+\bar{S}_1^*(Z)+\ldots\text{(b)}. \tag{5.11}$$

Here, essentially, $\bar{S}_1^*(Z)$ defines the thickness of the injectant region, while $\bar{R}(y)$ defines its shape. The expansions in (5.10), (5.11) are implied by the properties of subzone ⓑ as $Y \to \infty$ there. From (5.10) and (2.5a,b), the motion in ⓒ is controlled by the nonlinear equations

$$\left.\begin{aligned} \frac{d^2R_1^*}{dZ^2}V_1^{*2} &= -\left[1+\left(\frac{dR_1^*}{dZ}\right)^2\right]\frac{\partial P_1^*}{\partial\bar{x}} \\ &\quad +\left(\cos\alpha-\frac{dR_1^*}{dZ}\sin\alpha\right) \quad \text{(a)} \\ U_1^*\frac{\partial V_1^*}{\partial\bar{x}}+V_1^*\frac{\partial V_1^*}{\partial Z} &= \frac{dR_1^*}{dZ}\frac{\partial P_1^*}{\partial\bar{x}}+\sin\alpha, \quad \text{(b)} \end{aligned}\right\} \tag{5.12}$$

where $U_1^* = \partial\Psi_1^*/\partial Z$, $V_1^* = -\partial\Psi_1^*/\partial\bar{x}$.

The boundary conditions become

$$\left\{\begin{aligned} &V_1^* \sim 1+Z\sin\alpha,\ R_1^*(Z) \sim \frac{Z^2}{2}\cos\alpha \\ &\quad \text{as } Z\to 0 && \text{(5.13a)} \\ &P_1^* = 0 \text{ on } \bar{x}=0 \text{ and } \bar{x} = -\bar{S}_1^*(Z) && \text{(5.13b)} \\ &\Psi_1^* = 0 \text{ on } \bar{x} = -\bar{S}_1^*,\ \Psi_1^* = -2 \text{ on } \bar{x}=0 && \text{(5.13c)} \end{aligned}\right.$$

from matching with ⓑ and from (2.5c,d), (2.8).

We propose that $P_1^* \equiv 0$, which satisfies (5.13b) identically. Then (5.12a) implies that V_1^* is independent of $\bar{x}$, so that (5.12b) yields

$$V_1^* = V_1^*(Z) = (1+2Z\sin\alpha)^{1/2}. \tag{5.14}$$

Then (5.12a) yields the differential equation

$$(1+2Z\sin\alpha)\frac{d^2R_1^*}{dZ^2} = \cos\alpha-\sin\alpha\frac{dR_1^*}{dZ}$$

for $R_1^*(Z)$. The solution satisfying (5.13a) is

$$R_1^*(Z) = \cot\alpha[Z-(1+2Z\sin\alpha)^{1/2} \times \operatorname{cosec}\alpha+\operatorname{cosec}\alpha] \tag{5.15}$$

which defines the shape of the blown region. Also, integrating (5.14) to obtain Ψ_1^*, and applying (5.13c), we find that the thickness of the blown region is given by

$$\bar{S}_1^*(Z) = 2(1+2Z\sin\alpha)^{-1/2}. \tag{5.16}$$

The shape and thickness of the injectant region during this final stage (subzone ⓒ) are drawn in Fig. 6(a), for the particular inclined case $\alpha = \pi/6$, and in Fig. 6(b), for the horizontal case $\alpha = \pi/2$ where the bending effect (5.15) vanishes, of course, but the contraction (5.16) persists. Both the vertical and the

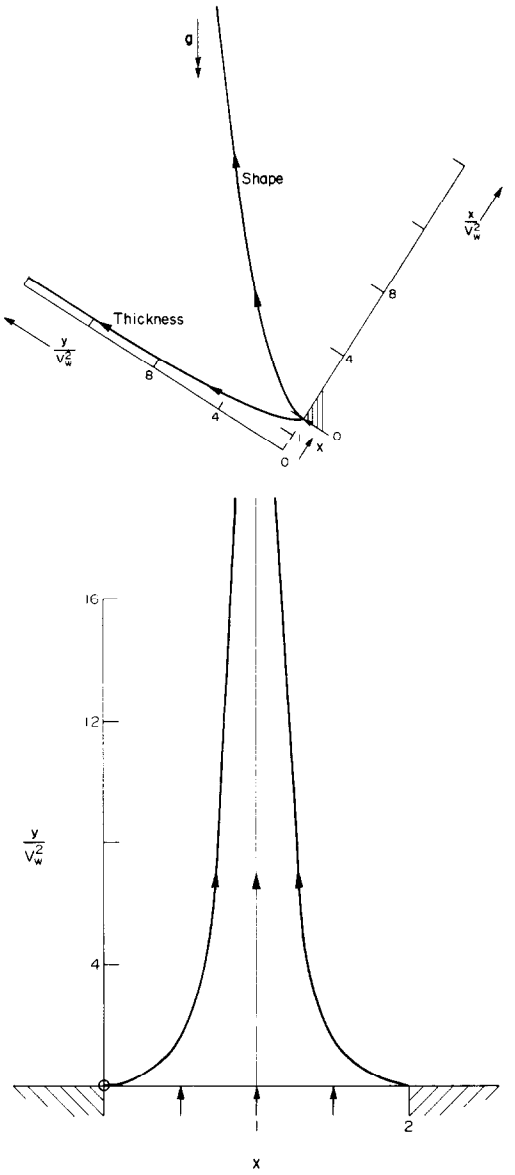

FIG. 6. (a) The shape of the upper dividing streamline [in (5.15)] and the thickness of the injectant region [in (5.16)] during the third stage ⓒ of the very strongly injected flow, for the inclined case $\alpha = \pi/6$. (b) The shape of the injectant region for a very strong, horizontal, convector.

horizontal cases are included (with some simplification) in the above analyses of the three subzones ⓐ, ⓑ, ⓒ; the vertical case merely repeats the exact solution of Section 3, of course, and the contraction effect from (5.16) vanishes. With the exception of the vertical case only, the injectant region contracts (proportionally to $Z^{-1/2}$) as Z increases still further, from (5.16), and the direction of the blown plume then approaches the vertical, from (5.15). The main physical balance of forces during the final stage ⓒ is as follows. (5.12a) is the playoff between buoyancy effects (the RHS, since $P_0^* = 0$) and the centrifugal effect normal to the injectant flow (the LHS) due to the turning of the strong blown injectant; (5.12b) expresses the balance of convective and buoyancy forces normal to the convector plate. Finally, the other regions (Fig. 1) of the problem also subdivide when V_w is large, since they are always driven by the properties of the injectant region, but we need not pursue their detailed features since the injectant properties above describe the principal attributes of the very strong convector heater.

6. FURTHER DISCUSSION

Like the solution in Section 3 for the vertical convector, the moderately strong blowing solutions for the horizontal and inclined convectors in Section 4 can be extended to deal with finite lengths of blowing. Similar phenomena to those of Section 3 then arise, with the original fluid in zone V being entrained into both the detached free-convection layer IV and the wall layer VI, so that again the motion in V is generally towards the convector plate. If, beyond the blowing length, the plate is maintained at a temperature different from T_w then the wall layer VI set up has a different character.

Thus the main attributes of strong convector heating are obtainable analytically for small (Section 4) or large (Section 5) V_w values if $0 < \alpha \leqslant \pi/2$ (Sections 4 and 5), and for any V_w value if $\alpha = 0$ (Section 3). For small V_w (moderately strong blow), the bounding streamline between the hot and the cold fluid takes a parabolic shape almost throughout, the exception occurring when the convector is only slightly inclined to the horizontal (there the shape changes fairly abruptly, to have a larger growth $\propto x^{2/3}$ when the convector is horizontal). As might be expected, the fluid blown from a moderately strong convector spreads only a small distance ($\propto V_w \ll 1$ for $0 \leqslant \alpha < \pi/2$) from the convector, at least until the endpoint of the blow (see below). In contrast, the penetration from a very strong convector is massive (Figs. 5, 6), the typical distance penetrated being $O(V_w^2)$ ($\gg 1$). Further, the adjustments of the very strongly injected flow, from its initial uniform state, perpendicular to the convector, to its final vertical form, involve a very gradual and subtle erosion of the blowing effect by the buoyancy forces (Section 5). The existence of the above analytic solutions for V_w small and V_w large also, to a certain extent, obviates the need for numerical solutions in the range $V_w = O(1)$, although the latter would complete the description of strong injection and would answer certain outstanding questions [e.g. does the injectant flow always approach the vertical if the blowing length is finite (as in Section 5); if so, how; and does the injectant plume contract (as in Section 5) in general?]. But perhaps more significant for practical purposes (in the heating of a room, for example) would be a study of strong blowing into a confined space rather than into the unconfined space that we have considered. A complicated circulating motion seems likely then, with the blown fluid being diverted by the boundaries into different parts of the space.

In order to determine the practical relevance of the theory, e.g. of the assumption of laminar flow, an experimental study of the convector heating would be desirable. However there seems to be a dearth of experimental work in this field, and what there is concerns the weak blowing situation, e.g. Lewis, Novotny and Yang [8]. It would certainly be interesting to see experiments performed to validate (or otherwise) our proposed structure. On the theoretical side, a stability analysis of the problem might shed some light on the mechanism of transition to turbulence. Again, however, we know of no work that relates directly to the convector problem where the main feature is the injectant plume I and its associated convection layers II and IV. There is an extensive literature on non-blowing free convection situations, and a thorough account with extensive references, including some on plume problems, is given by Pera and Gebhart [9]. Among many interesting and noteworthy points apparent from these stability investigations are that, for flows above heated plates, inclining the plate to the vertical destabilises the flow and, for a horizontal surface, the earliest onset of boundary-layer separation occurs at a local Grashof number (based on x rather than L_0) of about 5×10^5; of course, decreasing the inclination of the plate delays the onset of separation. These results are directly applicable to the free-convection layer VI. As far as the injectant fluid is concerned, we note that the buoyancy forces act in such a way as to cause it to flow in the (generally) more stable configuration of a vertical plume.

Finally it is of interest to consider numerical values associated with domestic (fan) convector heaters. These heaters typically operate in such a way that a 3kW fan heater raises the air temperature by about 40°C and blows the hot air out with a velocity in the range 50–500 cm s^{-1}. Thus, if we consider a 1.5kW heater with a 5cm deep outlet, and take air as our working fluid, we have say:

$$T_W = 40°C,\ T_\infty = 20°C,\ L_0 = 5\,\text{cm},$$
$$\nu_\infty = 0.1502\,\text{cm}^2\,\text{s}^{-1},\ g = 981\,\text{cm}\,\text{s}^{-2}\ \text{(and}\ \beta = 1/293).$$

Hence the Grashof number is about 3.7×10^5 and the dimensionless transpiration velocity V_w lies between 2.8 and 28; in other words, Gr is very large and V_w can be $O(1)$ or fairly large. Therefore the present work, and in particular that of Section 5, would certainly seem to be appropriate to the domestic convector.

Acknowledgement—The authors wish to thank Prof. D. B. Spalding and the referees for their comments on this paper.

REFERENCES

1. E. M. Sparrow and R. D. Cess, Free Convection with blowing or suction, *J. Heat Transfer* **83**, 387 (1961).
2. J. H. Merkin, Free Convection with blowing and suction, *Int. J. Heat Mass Transfer* **15**, 989 (1972).
3. J. F. Clarke, Transpiration and natural convection: the vertical-flat-plate problem, *J. Fluid Mech.* **57**, 45 (1973).
4. J. F. Clarke and N. Riley, Natural Convection induced in a gas by the presence of a hot porous surface, *Q. Jl Mech. Appl. Math.* **28**, 373 (1975).
5. E. Schmidt and W. Beckmann, Das temperatur and geschwindingkeitsfeld vor einer wärme adgebenden senkrechter platte bei natürlicher konvektion, *Tech. Mech. Thermo-Dynam., Berl.* **1**(10), 341 (1930).
6. S. Ostrach, An analysis of laminar free-convection flow and heat transfer about a flat plate parallel to the direction of the generating body force, N.A.C.A. Rep. 1111 (1953).
7. J. D. Cole and J. Aroesty, The blowhard problem—inviscid flows with surface injection, *Int. J. Heat Mass Transfer* **11**, 1167 (1968).
8. G. B. Lewis, J. L. Novotny and K. T. Yang, An experimental study of natural convection mass transfer along a vertical plate with surface injection, *J. Heat Transfer* **99**, 446 (1977).
9. L. Pera and B. Gebhart, On the stability of laminar plumes: some numerical solutions and experiments, *Int. J. Heat Mass Transfer* **14**, 975 (1971).

UN MODELE DE CONVECTEUR A PARTIR D'UNE PLAQUE PLANE

Résumé—On analyse la structure des champs d'écoulement laminaire et de température résultant d'une injection finie ("forte") et uniforme de fluide chaud sur une plaque plane verticale, horizontale ou inclinée. Les effects visqueux et les régions de changement de température sont déplacés à distance finie de la plaque et sont concentrés dans une mince couche détachée. Entre cette couche et la plaque, le fluide garde sa température de plaque et ilest déplacé vers le haut en s'éloignant de la plaque. Pour un soufflage modéré, les forces d'Archimède tendent à supprimer l'élargissement du fluide soufflé et on trouve que le fluide soufflé s'épanouit dans une région de forme parabolique, sauf quand le convecteur étant presque horizontal, l'élargissement croit de façon abrupte. Pour un soufflage reès important, l'injection pénètre sur une grande distance vers le convecteur avant que l'effet d'Archimède oblige le courant d'injection à tourner progressivement, à se contracter et à s'approcher enfin de la verticale.

MODELL EINER KONVEKTOR-HEIZUNG VON EINER FLACHEN PLATTE

Zusammenfassung—Es wird die Struktur der laminaren Strömung und der Temperaturverteilungen analysiert, die durch eine begrenzte ("starke") und gleichmäßige Einspritzung eines heißen Fluids auf eine senkrechte, waagerechte oder geneigte flache Platte entstehen. Die Zähigkeitseffekte und die Gebiete mit Temperaturänderung werden um eine gewisse Entfernung von der Platte fortbewegt und konzentrieren sich in einer schmalen abgelösten Schicht. Das ausgeblasene Fluid behält zwischen dieser Schicht und der Platte die Plattentemperatur und wird nach oben und von der Konvektorplatte weg transportiert. Bei nur mäßig starkem Ausblasen neigen die Auftriebskräfte dazu, die Verbreitung des ausgeblasenen Fluids zu unterdrücken, und es zeigt sich, das das ausgeblasene Fluid sich in einem Gebiet parabolischer Form ausbreitet mit Ausnahme des Falles, wenn der Konvektor beinahe waagerecht ist und die Ausbreitung schlagartig zunimmt. Im Gegensatz hierzu strömt das Fluid bei sehr starkem Ausblasen eine weite Strecke vom Konvektor weg, bevor die Auftriebskräfte die Fluidsäule allmählich ablenken, kontrahieren und letztlich in die Senkrechte bringen.

МОДЕЛЬ КОНВЕКТИВНОГО ТЕЧЕНИЯ У ПЛОСКОЙ ПЛАСТИНЫ

Аннотация — Анализируется структура ламинарного потока и распределений температуры при конечном («сильном») однородном вдуве горячей жидкости на вертикальной, горизонтальной или наклонной плоской пластине. Эффекты вязкости и теплопроводности проявляются на конечном расстоянии от пластины и концентрируются в тонком оттесненном слое. Между этим слоем и пластиной вдуваемая жидкость, сохраняющая температуру пластины, движется от пластины. При умеренном вдуве подъёмная сила препятствует растеканию вдуваемой жидкости. Найдено, что при этом вдуваемая жидкость распространяется в области параболической формы, за исключением случая почти горизонтального расположения пластины, когда растекание жидкости резко увеличивается. При очень сильном вдуве инжектируемая жидкость проникает на большое расстояние от пластины и только затем под действием подъёмной силы постепенно поворачивается, сужается и приближается к вертикальному направлению.